



Study the Gama ray attenuation parameters of some phosphate glass containing various amount of BCD

A.G. Mostafa, S.M. Salem, O.M. Yassin, and R.A. Abu-Gasser

Phys. Dept., Faculty of Science, Al-Azhar University, Nasr City, Cairo, Egypt.

ABSTRACT

By-Pass Cement Dust, as an industrial cement waste, was used here to prepare some gamma-ray shielding glasses aiming to protect people and environment from hazard radiations some phosphate glasses containing different amounts of by-pass cement dust have been prepared by the melt quenching method. The selected molecular composition was [(100-x) % P₂O₅ - (x) % By-Pass Cement Dust (where 30 ≤ x ≤ 60)]. The obtained experimental density and molar volume values were inspected and were then compared with those obtained empirically for the close packed structure of the corresponding compounds. These comparisons evidenced the short-range order and randomness character of the studied samples. Also X-ray diffraction analyses confirm the amorphous nature of all the prepared glasses.

The suitability of such glasses to act as gamma-ray shielding materials was also examined and a correlation between the chemical composition (By-Pass Cement Dust content) and gamma-ray attenuation behavior was established.

The electric and dielectric properties were thoroughly investigated.

The appearance of maxima and minima in the total conductivity by pass cement dust concentration dependence can be attributed to the mixed alkali – alkaline earth effect (K_2O & CaO).

INTRODUCTION:

Glasses are considered now as interesting solid materials due to their interesting properties and functional applications. Among various types of glasses, phosphate glasses are technologically important materials due to their interesting properties [1-3] but their poor chemical durability limits their diverse uses. It was found that the addition of at least 30 mol % metal oxides improves their chemical durability and act to attenuate γ -ray [4-6].

From another point of view, by-bass cement dust (BCD), as an industrial waste, represents a dangerous by-product of cement industry and it accumulated with huge amounts in Egypt. It causes various diseases, especially those related to human respiratory system [7]. According to the chemical analysis, such waste consists of various oxides (mainly, CaO , SiO_2 , Na_2O , K_2O and Fe_2O_3), where all these oxides can be introduced into the glass batches during the process of manufacturing different types of oxide glass [8,9]

It was found also that the use of different radioactive isotopes in various daily life fields is spread now, and it is not easy to protect ourselves from various hazard radiations prevailing through the environment. Knowing that, for different nuclear radiation sources, special shielding materials are required. Since glasses are usually transparent and

can be easy manufactured therefore, many articles have been published dealing with γ - ray attenuation of various glasses as transparent shielding materials [10-13].

However, in this article, it will be tried to prepare some phosphate glasses with different additives of BCD, as high as possible, in order to obtain chemically and mechanically stable glasses to consume the waste accumulation as well as to obtain low coast glasses. These glasses will be thoroughly investigated from gamma-ray shielding parameters point of view in order to investigate whether they can be used as transparent γ -ray shields or as capsulations for the radio-active wastes before interment underground or they may need some additives of any heavy metal oxides.

Experimental Details:

BCD was firstly analyzed by using X-ray fluorescence (XRF) and its chemical composition was presented in Table, [1].

Table (1), The chemical composition of the used BCD

Constituent	CaO	K₂O	SiO	Fe₂O₃	Al₂O₃	MgO	Na₂O	* LOI
Amount%	60.63	10.74	6.96	3.60	2.36	1.54	0.03	16.59

* LOI is loss of ignition

The selected glasses were prepared by weighting suitable amounts from ammonium di-hydrogen ortho-phosphate with different additives of the supplied BCD, so that when melted, they supply glasses having the following

composition [(70-x) P₂O₅ - x BCD, where 30 ≤ X ≤ 60 in steps of five mol% [11].

The glass batches were ground and mixed well in an agate mortar and they were then transferred into porcelain crucibles inserted into an electric muffle furnace at RT. The temperature of the furnace was raised up to 1100°C during 1 hr and kept at this temperature for 2 hrs. Melts were stirred several times during melting and were then poured between two copper plates in air. The obtained glass samples -just after solidifying- were transferred to the annealing furnace at 450°C for 2 hrs and the furnace was then turned off and left to cool to RT with a cooling rate of about 1.5°C/min.

The experimental density (ρ_{exp}) was measured by applying Archimedes principle, using carbon tetra-chloride (CCl₄) as an immersion liquid. In such principle, a sample was weighted in air (M_a) and in CCl₄ (M_l), and then (ρ_{exp}) can be calculated by using equation (1) [12],

$$\rho_{exp} = \left[\frac{M_a}{M_a - M_l} \right] \rho_l \quad (1)$$

The experimental molar volume values ($(V_m)_{exp}$) were then obtained by using equation (2) [12],

$$(V_m)_{exp} = \frac{M_m}{\rho_{exp}} \quad (2)$$

Where M_m is the main molecular weight in (g/mol) of a glass sample.

The empirical density values (ρ_{emp}) were also calculated by using the following relation [13],

$$\rho_{\text{emp}} = \sum \rho_i X_i \quad (3)$$

where ρ_i are the densities of the oxides forming a glass sample and X_i are the mole fractions of each oxide.

The empirical molar volume $(V_m)_{\text{emp}}$ values were then obtained by using equation (2), but with replacing ρ_{exp} by ρ_{emp} [13].

XRD patterns were obtained by using Rigaku-RINT 2100, outfitted with Cu k_α radiation of $\lambda = 0.1541$ nm and the operating current and voltage were 300 mA and 50 KV, respectively.

Gamma-ray attenuation parameters (total mass attenuation coefficient $(\mu_L/\rho)_m$, half value layer (HVL) and mean free path (MFP) of a glass sample were then calculated by applying WIN-XCOM program, based on the mixture rule [13].

Different amount of BaO as heavy metal oxide were then introduced at the expense of P_2O_5 in the samples $[(50-x) P_2O_5 - xBaO - 50 BCD]$, where $0 \leq X \leq 20$ in steps of five mol%. The linear attenuation coefficients of the studied glass system were measured in narrow beam transmission geometry. The experimental setup of such geometry was exhibited in Ref. [14].

For electrical measurements, the obtained solid glasses were polished from both sides in order to obtain optically flat disk shape samples of 8 mm diameter and 1 mm thickness. The disks were then coated from both sides with an air-drying silver paste to achieve good electrical contact. The measurements were carried out by using a computerized Stanford LCR bridge

model SR 720 at four fixed frequencies [0.12, 1, 10, 100 kHz]. All measurements were performed in the temperature range from RT up to 250°C.

RESULTS AND DISCUSSION.

1- Confirmation of the amorphous nature

All the obtained solid samples were examined visually where they appeared transparent and free of inclusions and air bubbles, that is they appeared in good and homogeneous glassy phase. In spite of this, they were examined by using XRD analysis and the obtained patterns are exhibited in Fig.

(1) Where all patterns are found free of any sharp crystalline peak [15]

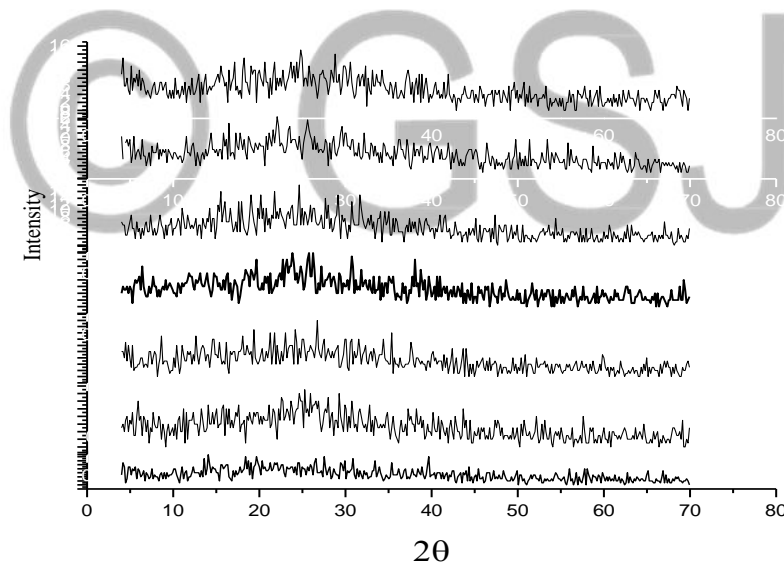


Fig. (1) The obtained XRD patterns of all glasses

Both the obtained density values (ρ_{exp} & ρ_{emp}) are listed in Table (2), for comparison as a function of BCD content, where it is seen that both ρ_{exp} & ρ_{emp} increased gradually with the gradual increase of BCD.

Table (2) The obtained ρ_{exp} and ρ_{emp} values as a function of BCD content.

BCD mol%	30%	35%	40%	45%	50%	55%	60%
ρ_{exp} (gm/cm ³)	1.92	2.35	2.47	2.62	2.70	2.85	3.16
ρ_{emp} (gm/cm ³)	2.70	2.75	2.80	2.85	2.90	2.95	3.20

Since the molar volume is directly related to the internal spatial structure of materials, it is suitable to exhibit also the change of the molar volume as a function of BCD of the studied glasses. Both molar volume values ($V_{\text{m emp}}$ & $V_{\text{m exp}}$) are exhibited in Table (3), as a function of BCD.

Table (3) The calculated V_{exp} and V_{emp} values as a function of BCD content.

BCD mol%	30%	35%	40%	45%	50%	55%	60%
V_{exp} (gm/cm ³)	59.95	47.36	43.16	39.06	36.26	32.86	28.28
V_{emp} (gm/cm ³)	42.82	40.43	38.12	35.90	33.75	31.68	27.87

It is observed that both molar volume values show approximately gradual decrease. The observed variations of both density and molar volume values may be due to the introduced BCD which contains various positive cations. These cations fill mostly the network vacancies, and in turn decrease the internal free volume.

Accordingly, the density is logically increased while the molar volume decreased. In addition, it can be stated that, the higher empirical density and the lower empirical molar volume values than these obtained experimentals

can be taken as confirmation for the amorphous nature and the short-range order character of the studied samples [16].

2- Gamma-Ray Attenuation parameters:

Until now, the majority of nuclear radiation shields in nuclear facilities are formed **mainly** of layers of different types of concrete with various compositions and densities as well as layers of lead sheets. But considerable variations of water content in concrete induces high uncertainty factor in calculating their attenuation coefficients due to the continuous variations of their densities, while lead is characterized by its toxicity. Moreover, both concrete and lead are opaque to visible light [17]. But materials that have to be used for shielding must be of stable density and composition as well as they preferably to be transparent. In this regard, glasses are promising materials, since they are usually transparent and easy manufactured.

Berger and Hubbell [18] at 1987 have developed a program called X-COM program for calculating the total mass absorption coefficients or the photon interaction cross-sections for any element, compounds or mixtures at various photon energies from 1 keV to 100 GeV. Recently, X-COM was transformed to the Windows platform by Gerward et al. [19] at 2001 where it is named Win-XCom. With the development of such program, it becomes easy to calculate the total mass attenuation coefficient for different shielding materials. However, it is of interest to check the ability of the studied glasses to act as transparent shielding materials and to investigate whether their

compositions are suitable for this purpose or they may need to introduce some heavy metal oxides into their networks.

On the other hand, the linear attenuation coefficient of the studied glasses have been measured experimentally by applying the narrow beam transmission geometry, where if an incident γ -ray photon of intensity (I_0) have passed through a sample of thickness (x) the exit photon intensity (I) can be calculated by using the following equations

$$\mu_L = \ln\left(\frac{I_0}{I}\right) \quad (4)$$

The experimental mass attenuation coefficient can be calculated by using both the measured μ_L & ρ_{exp} as follows equation,

$$\mu_m = \ln(I_0/I) / \rho_x \quad (5)$$

On the other hand the value of the total mass attenuation coefficient of the studied glasses can be calculated by applying Win-X-COM program (based on the mixture rule) by using equation (6) [20,21].

$$\left(\frac{\mu}{\rho}\right)_m = \sum_i^n w_i \left(\frac{\mu}{\rho}\right)_{mi} \quad (6)$$

Where $(\mu/\rho)_m$ is the total mass attenuation coefficient of a sample, $(\mu/\rho)_{mi}$ is the total mass attenuation coefficient of the composing elements of such sample and w_i is the fractional weights of each element in the studied sample.

Theoretical values for the total mass attenuation coefficient can be found in the tables prepared by Hubbell and Seltzer [20].

The linear attenuation coefficients (μ_L) can be then calculated and the obtained values are correlated to the half value layer (HVL) according to equation (7),

$$\text{HVL} = 0.693 / \mu_L \quad (7)$$

Where HVL is the thickness of the material that decreases the intensity of the incident photon to its half value.

The Mean free path (MFP) of a gamma-ray photon (λ), can be also calculated by using equation (8),

$$\lambda \text{ (MFP)} = 1/\mu_L \quad (8)$$

Where (λ) is the mean distance that a photon can travel between any two successive interactions of the photon with matter.

Fig. (2) shows the variation of the calculated μ_m values for the studied glasses at different low γ -ray energies as a function of BCD content. It is found that μ_m show generally, slight linear increase with the increase of the weight fraction of BCD at the expense of P_2O_5 . This may be due to the gradual increase in the density of the investigated glass samples. Such increase in density act to increase the photon interaction probability at these energies which indicates better shielding properties. The onset plotted between μ_m

and BCD content at γ -ray energy at 356 Kev show obviously such variations.

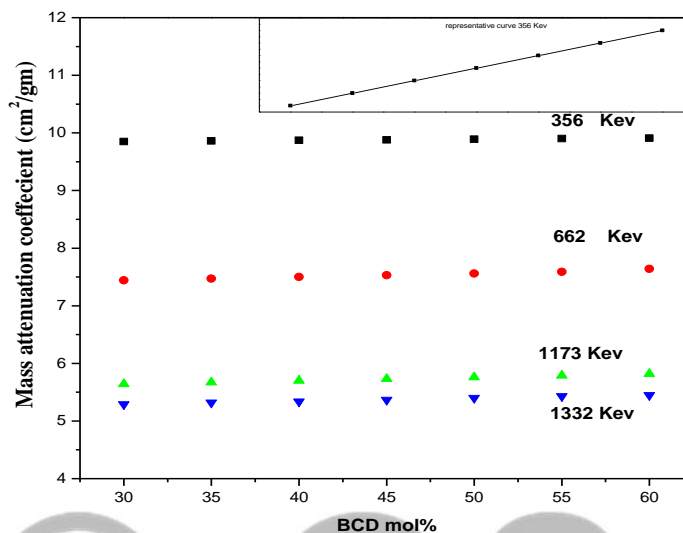


Fig. 2. The variation of μ_m as a function of BCD content at different low γ – ray energies

The numerical values of the calculated μ_m at different energies are summarized in Table (4).

The linear attenuation coefficient (μ_L). represents the fraction of photons removed from a monoenergetic beam per unit thickness of a material and it is expressed in units of cm^{-1} . Fig. (3) Shows the variation of linear attenuation coefficient as a function of BCD content, at different low gamma-ray energies. It appeared that, μ_L increases with the increase of BCD, which may be due also to the gradual increase of density.

Table 4. The variation of the Mass attenuation coefficient as a function of BCD content at relatively low γ -ray energies

BCD mol%	Density gm/cm ³	μ_m (cm ² /gm) X (10 ⁻²)			
		356 Kev	662 Kev	1173 Kev	1332 Kev
30	1.93	9.851	7.44	5.64	5.29
35	2.35	9.86	7.47	5.67	5.32
40	2.48	9.87	7.50	5.69	5.34
45	2.62	9.88	7.53	5.72	5.37
50	2.71	9.89	7.56	5.76	5.40
55	2.85	9.9	7.59	5.79	5.43
60	3.16	9.91	7.64	5.82	5.45

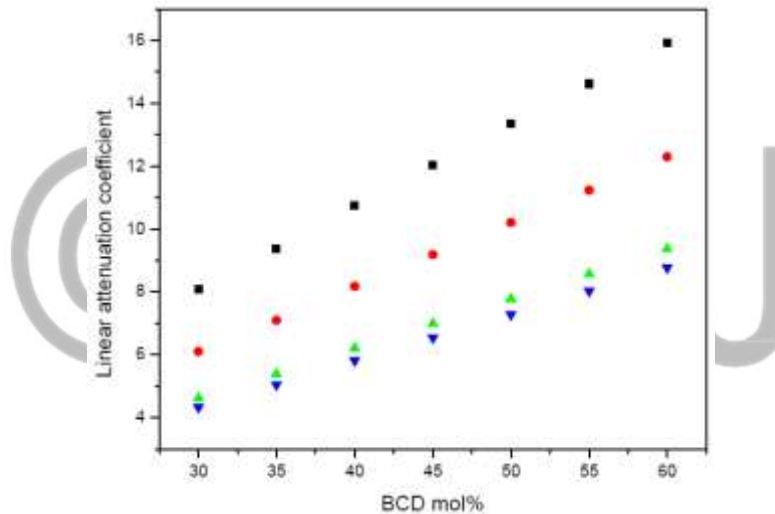


Figure 3. The variation of the μ_L values as a function of BCD content at different γ -ray energies

Fig. (4) shows the behavior of HVL for the studied glasses as a function of BCD, at various low gamma-ray energies. This figure indicates that the HVL decreases with the increase of the weight fractions of BCD. This may be due to the gradual increase of the linear attenuation coefficient and the

densities of the studied glass samples Also, the onset in this figure show obviously such variation.

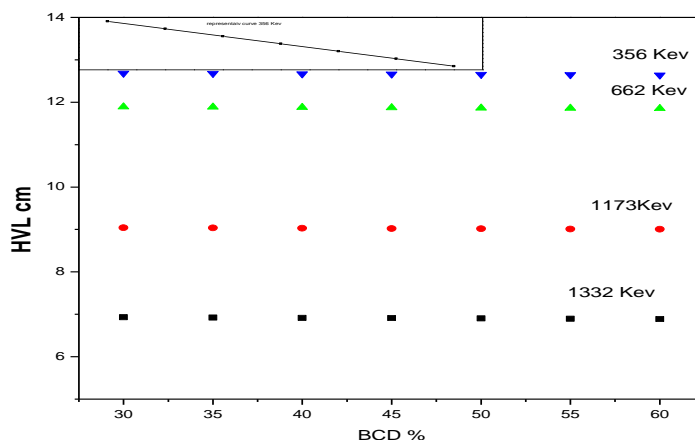


Figure 4. The variation of the HVL as a function of BCD content at relatively low γ – ray energies

The numerical values of the calculated HVL at different low γ –ray energies are summarized in Table (5).

Table 5. The calculated HVL as a function of BCD, at relatively low gamma-ray energies

BCD (mol%)	Density (gm/cm ³)	HVL (cm)			
		356 Kev	662 Kev	1173 Kev	1332 Kev
30	1.92	6.93	9.04	11.89	12.68
35	2.35	6.92	9.03	11.88	12.67
40	2.47	6.91	9.02	11.87	12.66
45	2.62	6.9	9.01	11.86	12.65
50	2.70	6.89	9	11.85	12.64
55	2.85	6.88	8.99	11.84	12.63
60	3.16	6.87	8.98	11.83	12.62

The MFP is the average distance traveled by a moving photon between two successive impacts. Such value can be used to describe the effectiveness of the studied shields. Fig. (5), shows the behavior of the MFP as a function of BCD content, at various low gamma-ray energies. This figure indicates that MFP decreases with the increase of the weight fractions of BCD, which may be due to the gradual increase of the molar volume of the studied glass samples, and hence the gradual increase of μ_L [19].

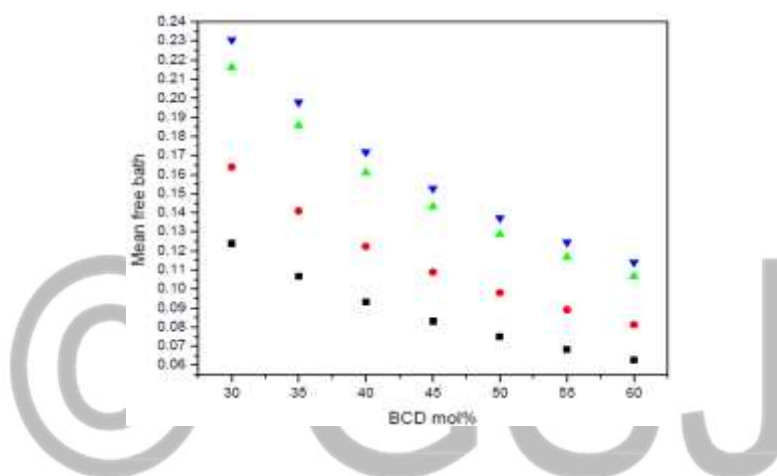


Figure 5. The variation of MFP, as a function of BCD content

It is suitable to compare the obtained values (exp. & Theo.) of the linear attenuations coefficients for the studied glasses

It can be observed from Table. (6) that the experimental linear attenuation coefficient exhibits approximately gradual increase as BCD was increased, but it shows approximately gradual decrease as the γ - ray energy was increased.

Table. (6) The experimental & theoretical linear attenuation coefficient

BCD%	30%	35%	40%	45%	50%	55%	60%
μ_{exp}	0.0762	0.0942	0.0942	0.1122	0.12	0.1302	0.1821
μ_{theo}	0.065	0.085	0.105	0.126	0.144	0.16	0.17

It can be observed from Fig. (6) that the comparison between the exp. & theo. linear attenuation coefficient of the studied of glasses exhibits approximately gradual increase as BCD was increased, it appeared also that both variations are very near to each other and the observed difference may be due to the used industrial waste.

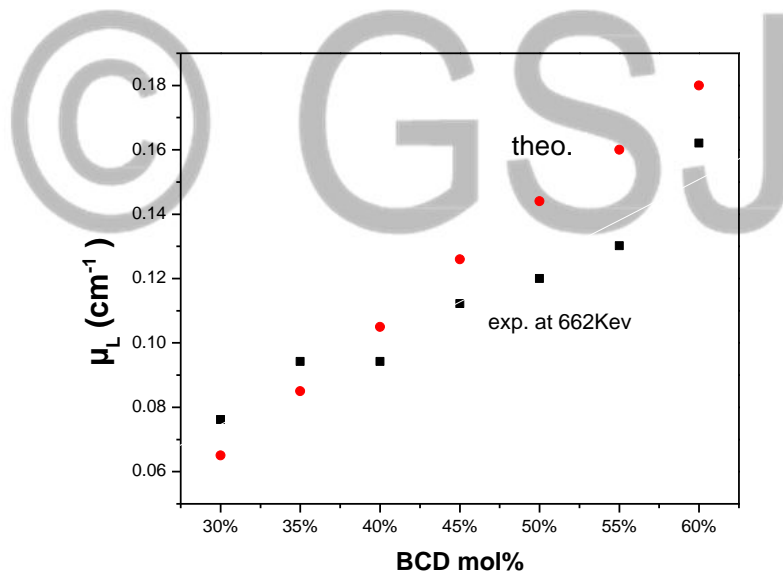


Figure 6. Comparison between the exp. & Theo. linear attenuation of glasses.

The total mass attenuation coefficient of the samples containing BaO

Noticing that, the studied glasses contain no any heavy metal cations (only phosphorous and BCD constituting cations), and it is supposed that, if some heavy metal cations are introduced into their network, this may improve their gamma-ray attenuation parameters. However, these parameters will be checked again when different amounts of BaO are introduced into their networks. The mass attenuation coefficients as a function of γ - ray energies for different BaO concentrations are represented in Table. (6).

Table 6. The variation of the Mass attenuation coefficient as a function of BaO content at relatively low γ - ray energies.

BaO mol%	$\mu_m (\text{cm}^2/\text{gm}) \times (10^{-2})$			
	356 Kev	662 Kev	1173 Kev	1332 Kev
0	10.1	7.68	5.83	5.47
5	10.3	7.69	5.81	5.44
10	10.5	7.70	5.78	5.41
15	10.7	7.71	5.75	5.39
20	10.9	7.72	5.72	5.37

It can be observed from Fig. (7) that the mass attenuation coefficient exhibits approximately gradual increase as BaO was increased, but it shows approximately gradual decrease as the γ - ray energy was increased. This behavior shows good confirmation that the introduced BaO act to increase the mass attenuation coefficient. It appeared also that the studied glass samples exhibit high shielding efficiency at low γ - ray energies and their efficiency decreased as the γ - ray energy increased.

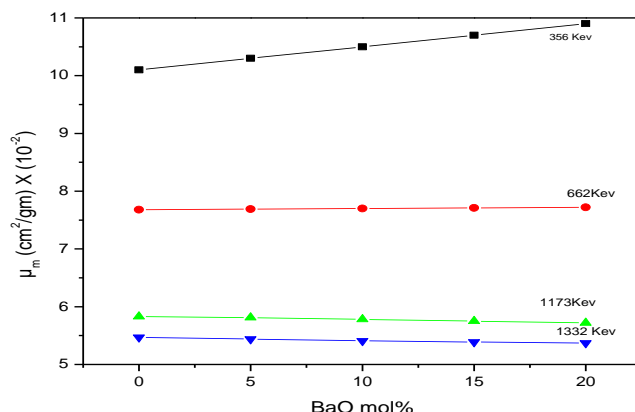


Figure 7. The variation of μ_m of glasses containing different concentration of BaO.

It can be observed from Table. (7) that the comparison between the exp. & Theo. linear attenuation coefficient of glasses containing heavy metals exhibits also approximately gradual increase as BaO was increased.

Table (7) Shows the obtained values of the Theo. & exp. linear attenuation coefficient of glasses containing BaO

BaO %	5	10	15	20
Theo. μ	.1122	.1211	.1302	.1425
exp. μ	.1224	.1323	.1432	.1546

Fig. (8) show a comparison between the exp. linear attenuation coefficient of glasses containing BaO and glass without BaO. And both variations exhibits approximately gradual increase as BaO was increased. it can be observed also that the linear attenuation coefficient of the glasses containing BaO are higher than those containing no BaO.

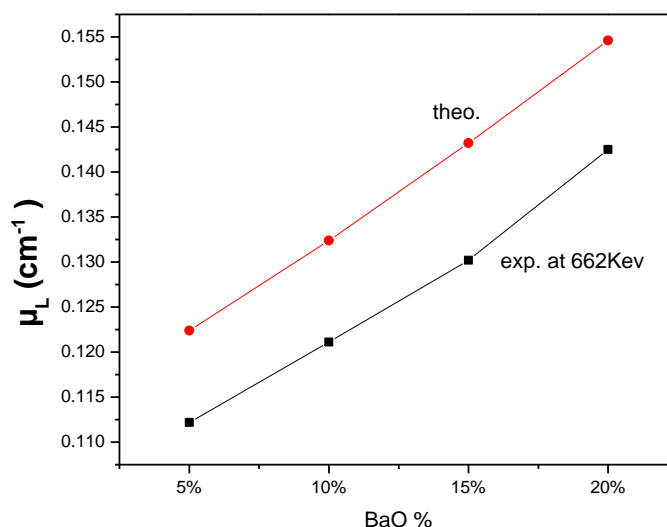


Figure 8. Comparison between exp. linear attenuation of the glasses containing different amounts of BaO content.

Generally, these results indicated that the studied glasses are good attenuators for gamma photons and they represent promising gamma-ray shielding materials due to their high mass attenuation coefficient and their low half value layer, especially when some BaO has introduced into their glass networks.

3. conductivity

It is well known fact that, the interaction of gamma-ray with matter can induce some electrical charges. These charges must be readily released from the shielding material directly. Therefore checking the semiconductor properties of such glass is of interest. The dc conductivity values were then calculated from the fitting of the experimentally obtained σ_T data with equa-

tion (9) and the obtained data are then plotted in Fig. (9) as a function of BCD content.

$$\sigma_{dc} = \sigma_0 \exp (-\Delta E_a/kT) \quad (9)$$

where σ_0 is the pre-exponential factor, ΔE_a is the activation energy, k is Boltzmann constant and T is the absolute temperature.

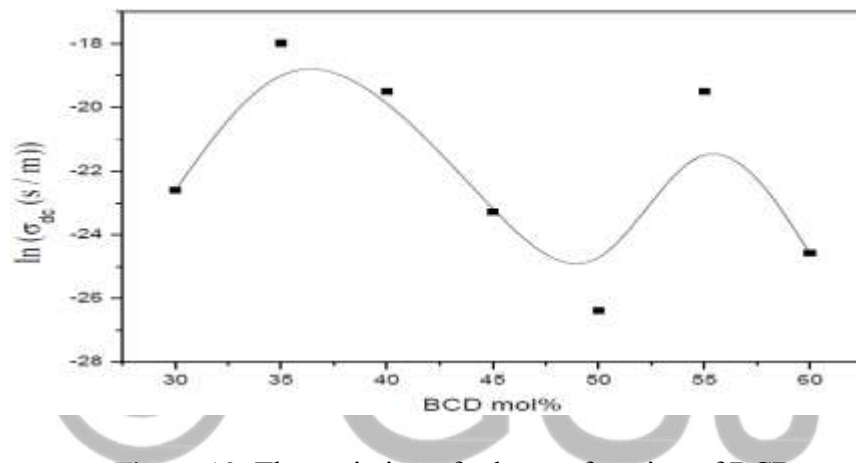


Figure 10. The variation of σ_{dc} as a function of BCD

It is seen that the variation of σ_{dc} is a non-linear behavior and a maxima and a minima are exhibited at 35 and 50 mol% BCD, corresponding to CaO concentrations of 21 and 33 mol% respectively and the amounts of K_2O are 3.3 and 6.05 mol% respectively. It can be supposed that the observed non-linear behavior may be due to the mixed alkali-alkaline earth effect [20, 23].

The dc electrical activation energy (ΔE) can be then calculated from the slopes of the obtained straight lines of the studied sample at relatively high temperatures (where the dc conductivity is dominant) according to Arrhenius equation (equation 8), The variation of the activation energy with BCD is exhibited in Fig. (10), where this variation shows approximately the reverse

behavior of the dc conductivity and such trend was expected to be logic [24, 25].

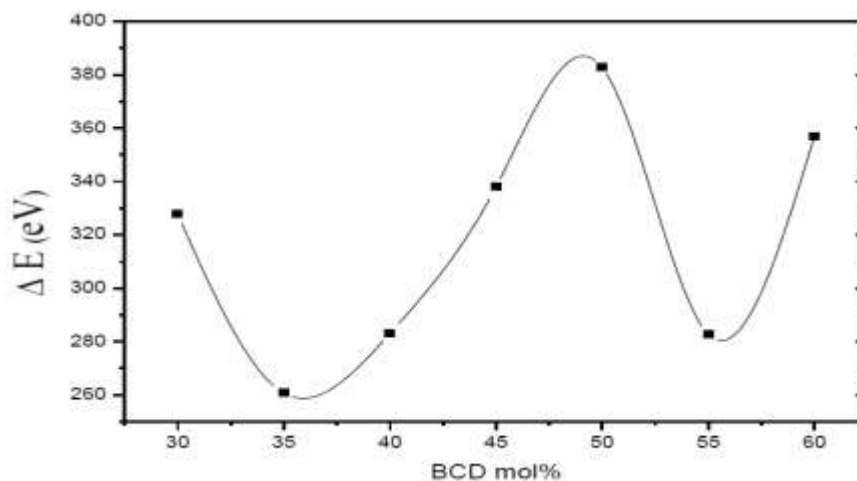


Figure 10. The variation of ΔE values as a function of BCD

CONCLUSION:

According to the obtained results and the proposed discussion in this study, the following conclusions can be drawn :

- 1- Some phosphate glasses with different additives of BCD (industrial iron wastes) as high as 60 mol%, can be prepared, where these glasses are environmentally friends.
- 2- The visual examination showed pure glassy phase of all the prepared samples, and the XRD analysis confirm their amorphous nature as well as their randomness structure.

- 3- The densities of the studied glasses are found to increase gradually as BCD was gradually increased.
- 4- The studied glasses represent good attenuators for γ –photons and promising gamma-ray shielding material due to their high mass attenuation coefficient and their low half value layer (HVL) only at low gamma-ray energies.
- 5- The introduced of some heavy metal cation improve all the gamma-ray shielding parameters.
- 6- all the studied glasses show semi conduction properties and they can release any charge that can be formed on these shielding glasses.

REFERENCES

1. R. Mercier, J. P. Malugani, B. Fahys, and G. Robert, Solid State Ionics, 5 (1981) 663.
2. M. Wada, M. Mcnetrier, A. Le Vasseur and P. Hagenmuller, Mater. Res. Bull., 18 (1983) 189.
3. H. Mori, H. Matsuno and H. Sakata, J. Non-Cryst Solids, 276 (2000) 78.
4. G. D kattak, E. E. Khfaja, L. E. Wenge, D. J. Thompson, M. A. Said, A. B. Hallak and M. A. Daous, J. Non-Cryst. Solids, 194 (1990) 1.
5. A. saeed, R.M. El-Shazly, Y.H. Elbashar, and M.M. El-Okr, Radiat. Phys. Chem., 102(2014)167.
6. H.A. Saudi, A. Abd-Elalim, T.Z. Abou-Elnasr, A.G. Mostafa, Nature and Science, 13(11) (2015)139.
7. A.M. El-Khayatt, A. M. Ali and V.P. Singh, Nucl. Inst. Methods Phys. Res. (A), 735 (2014) 2014.

8. S. Grandi, P. Mustarelli, A. Magistris, M. Gallorini and E. Rizzio, J. Non-Cryst. Solids, 303 (2002) 208.
9. Y. M. Mustafa and A. AL. Adway, Phys.Status Solid (A),179 (2000) 83.
- 10.E. Metwalli, M. Karabulut, D. L. Sideborton, M. Mrsi and R.K. Brow, J. Non-Cryst. Solids, 344 (2004) 128.
- 11.A. A. Bendary, Ph. D. Thesis, Phys. Dept. Faculty of Science, AL-Azhar Univ., Egypt, (2014).
- 12.S. Duhan, S. Sanghi, A. Agarwal, A. Sheoran and S. Rani, Physica B, 404 (2009) 1648.
- 13.N.T. Sheldon Landsberger, "Measurement & Detection of Radiation" 4th edition, France (2015).
- 14.G. S. M. Ahmed, A. S. Mahmoud, S. M. Salem, T.Z. Abo-Elnaser .American Journal of Physics and Applications. 3(4)(2015)112.
- 15.H.S. Chen, J. Non-Cryst. Solids, 27 (1978) 257.
- 16.S. Wuy, X. Wei, X. Wang, H. Yang and H. Gao, J. Mater. Sci. & Technol., 26 (5) (2010) 472.
- 17.J.F. Krocher, R.E. Browman "Effects of Radiation on Materials and Components", Reinhold, New York, (1984).
- 18.J. Berger, J.H. Hubbell, NBSIR (1987), 87.
- 19.L. Gerward, N. Guilbert, K.B. Jensen and H. Levring, Radiat. Phys. Chem., 60 (2001) 23.
- 20.J.H. Hubbell, S.M. Seltzer, NISTIR 5632 (1995).

21. A.M. Abdel-Ghany, A.M. Zoulfakar, T.Z. Abo-Elnaser, M.Y. Hassan and A.G. Moustafa, American Journal of Phys. and Applications, 3(6) (2015) 208.
22. A.M. Abdel-Ghany, M.S.S. Saad, I.I. Bashter, T.Z. Amer, S.M. Salem and A.G. Mostafa, Nature and Science, 12(2014)162.
23. B. Qian Xiaofeng Liang, Shiyuan Yang, Shu He and Long Gao, J. Molecular Structure, 1027 (2012) 31.

© GSJ